

# Crystallization of Poly(butylene terephthalate) and Its Blends with Polyarylate

J. Runt,\* D. M. Miley,<sup>†</sup> X. Zhang, K. P. Gallagher, K. McFeaters, and J. Fishburn

Polymer Science Program, Department of Materials Science and Engineering,  
The Pennsylvania State University, University Park, Pennsylvania 16802

Received August 26, 1991; Revised Manuscript Received December 9, 1991

**ABSTRACT:** In this paper we explore the crystallization kinetics of poly(butylene terephthalate) (PBT), poly(ethylene terephthalate) (PET), and miscible blends of PBT with a polyarylate based on Bisphenol A and a 75/25 mole ratio of isophthalic and terephthalic acids. For PBT, a regime II  $\rightarrow$  III transition is indicated near 210 °C ( $\Delta T \sim 30$  °C) and the fold surface free energy ( $\sigma_e$ ) was found to be in the range of 57–75 erg/cm<sup>2</sup>. This leads to a work of chain folding ( $q$ ) of  $\sim 3$ –5 kcal/mol folds. Analysis of the crystallization data of van Antwerpen and van Krevelen for PET shows that crystallization occurs in regime II across a wide range of  $T_c$ .  $\sigma_e$  was estimated to be  $\sim 140$  erg/cm<sup>2</sup> and  $q \sim 10$  kcal/mol from their data. These values are roughly twice that of PBT, consistent with the longer flexible segments in the PBT repeat unit. Crystallization data for three PBT/PAr blends was analyzed using a modified Lauritzen–Hoffman method and compared to that of pure PBT.

## 1. Introduction

We have been interested in various aspects of miscible blends of poly(butylene terephthalate) (PBT) and a polyarylate, particularly the existence and nature of a crystal–amorphous interphase<sup>1</sup> and the role of transesterification during melt processing on properties.<sup>2</sup> In this paper we focus on the kinetics of crystallization of PBT as well as PBT in blends with polyarylate. Spherulitic growth rate data are analyzed using the Lauritzen–Hoffman approach<sup>3</sup> or a modification thereof for the blends. Crystallization regime behavior and thermodynamic parameters such as the fold surface free energy and the work of chain folding are discussed in light of our current understanding of polymer crystallization.

## 2. Experimental Section

**A. Materials and Preparation.** The PBT and polyarylate (PAr) used in this study were provided by Hoechst Celanese Corp. The PBT was of relatively high molecular weight; it had an intrinsic viscosity of 1.42 dL/g in a 40/60 wt % mixture of 1,1,2,2-tetrachloroethane (TCE) and phenol (Ph) at 30 °C yielding  $\bar{M}_w = 83\,000$  and  $\bar{M}_w/\bar{M}_n = 1.9$ . The polyarylate under consideration here is based on Bisphenol A and isophthalic and terephthalic acids (in the mole ratio of 75/25 isophthalic acid/terephthalic acid) and had an intrinsic viscosity of 0.60 dL/g at 30 °C in tetrahydrofuran. This translates into  $\bar{M}_v \sim 36\,000$ .<sup>5</sup>

Blends were prepared using the solution precipitation procedure of Kimura et al.<sup>6</sup> PBT and PAr (2 g of each) were each dissolved in 100 mL of TCE/Ph (40/60). Each solution was stirred at 80 °C for 4 h. This reflux procedure was repeated three times. The final product was dried under vacuum at temperature in excess of the calculated blend  $T_g$  (taking into account PBT crystallinity). Kimura et al.<sup>6</sup> and others (e.g., ref 7) have provided evidence for the miscibility of these two polymers.

**B. Characterization.** Measurement of melting points was accomplished with a Perkin–Elmer differential scanning calorimeter, DSC-7. A heating rate of 20 °C/min was used in all cases, and the melting endotherm was defined by base line constructed from 135 °C to a temperature above which no melting was observed. In order to avoid difficulties with low polymer thermal conductivity,<sup>8</sup> sample sizes were in the range of 0.2–0.3 mg, unless otherwise specified. All measured values reported are based on an average of a minimum of two DSC scans. Pure

indium and lead were used as reference materials to correct temperature values of heats of fusion.

Isothermal spherulitic growth rates of PBT and its blends with PAr were determined over a range of crystallization temperatures using an Olympus BHSP-300 optical microscope and a Mettler FP82 hot stage. Films were produced from the solution-precipitated material by placing a small quantity of the precipitate (which was in the form of a coarse powder) between two pieces of Teflon-coated aluminum foil and heating to  $\sim 340$  °C under minimal pressure and for a short time (several seconds). These films were then melted at 250 °C in the hot stage for 5 min in an attempt to eliminate remnants of their previous thermal history and then rapidly cooled to the desired crystallization temperature ( $T_c$ ). In order to minimize degradation at high temperatures, all samples were dried and kept desiccated prior to use. We were concerned about the possibility for transesterification during this high-temperature exposure, but results from <sup>1</sup>H NMR experiments indicate that no measurable reaction had occurred. At each crystallization temperature the average spherulite radius was determined at approximately 10 different time intervals. Due to the high nucleation density and small spherulite size, it was necessary to use a somewhat unconventional and tedious approach for the determining average spherulite size at a particular crystallization time. Each sample was quenched into ice water (i.e., below  $T_g$ ) after the elapsed crystallization time at  $T_c$  and then viewed and photographed at the highest magnification possible. The average spherulite radius at each time interval was determined using a Zeiss digital analysis system from an average of approximately 30 spherulites. The measurement of an average spherulite size is a reasonable technique to measure growth rate only if all of the spherulites nucleate instantaneously, as was witnessed here.

## 3. Results and Discussion

**A. Poly(butylene terephthalate).** Isothermal spherulitic growth rates of PBT and PBT in blends with PAr over a range of  $T_c$ 's are shown in Figure 1. As expected, the growth rate of PBT spherulites in the blends is lower than that of pure PBT and proportional to the PAr concentration. Since the quenching technique used to gather the growth rate data was unconventional, there was some concern initially about whether the data was reasonable or not. The results of our research and the limited PBT spherulitic growth rate information available in the literature<sup>9–11</sup> are in good correspondence, especially considering possible differences in molecular weight. It should be noted, however, that the errors introduced by

<sup>†</sup> Present address: Kraft General Foods, Glenview, IL 60025.

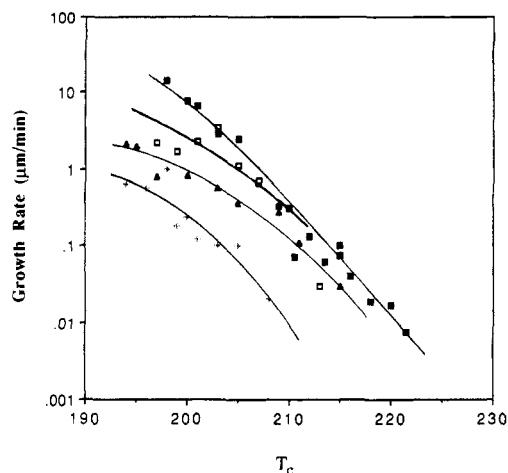


Figure 1. Spherulitic growth rates of PBT and PBT/PAr blends.

Table I  
Nucleation Constants and Preexponential Factors for PBT and PBT/PAr Blends

	regime	$K_g \times 10^{-5} (K^2)$	$G_0, \text{cm/s}$
PBT	II	0.53	$8.3 \times 10^{-4}$
	III	1.86	62
PBT/PAr (90/10)		1.27	0.27
PBT/PAr (80/20)		0.97	$6.1 \times 10^{-2}$
PBT/PAr (70/30)		1.69	2.1

using this approach are larger than those normally encountered in the measurement of spherulitic radii in situ at  $T_c$  and so care must be taken not to overinterpret the experimental data.

The spherulitic growth rate of ( $G$ ) of PBT was analyzed using the Lauritzen-Hoffmann expression<sup>3</sup>

$$G = G_0 \exp[-U^*/R(T_c - T_\infty)] \exp[-K_g/T_c(\Delta T)f] \quad (1)$$

where  $U^*$  is the transport activation energy,  $R$  the gas constant,  $T_\infty$  the hypothetical temperature below which all viscous flow ceases,  $K_g$  a nucleation parameter,  $\Delta T$  the degree of supercooling, and  $f$  a correction factor to account for the variation in  $\Delta H_f^\circ$  (the perfect crystal heat of fusion) with temperature,  $f = 2T_c/(T_m^\circ + T_c)$ . Growth rates at relatively low degrees of supercooling (the only ones accessible here) are well-known to be relatively insensitive to the values of  $U^*$  and  $T_\infty$  employed in eq 1, and the "universal" values of  $U^* = 1500 \text{ cal/mol}$  and  $T_\infty = T_g - 30 \text{ K}$  were used in all calculations. The nucleation constant,  $K_g$ , takes the form

$$K_g = nb\sigma\sigma_e T_m^\circ / \Delta H_f^\circ k \quad (2)$$

where  $b$  is the thickness of a monomolecular layer,  $\sigma$  and  $\sigma_e$  are the lateral and end surface free energies, respectively,  $T_m^\circ$  is the equilibrium melting point, and  $k$  is the Boltzmann constant.  $n$  takes on a value of 4 in regime I or III and a value of 2 in regime II. It is often most convenient to rearrange eq 1 as

$$\log G + \frac{U^*}{2.3R(T_c - T_\infty)} = \log G_0 - \frac{K_g}{2.3T_c(\Delta T)f} \quad (3)$$

and view the growth rate data in the form of a plot of the left-hand side of eq 3 vs  $1/T_c(\Delta T)f$ , with the slope  $= -K_g$ . From above, it is evident that  $K_g(\text{III})/K_g(\text{II}) = K_g(\text{I})/K_g(\text{II}) = 2$ . Thus, regime transitions should be readily apparent from slope changes in such plots. In fact, regime I  $\rightarrow$  II and II  $\rightarrow$  III transitions have been established for a growing number of polymers.<sup>12</sup>

Before proceeding with quantitative analysis of the crystallization behavior, the equilibrium melting point of

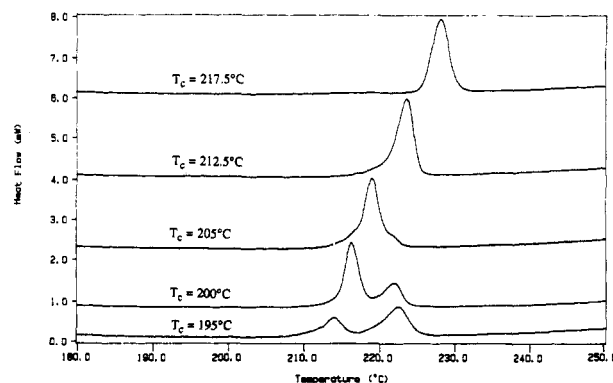


Figure 2. Melting behavior of isothermally crystallized PBT (heat rate = 20 °C/min).

PBT must be established as accurately as possible since the thermodynamic parameters derived from the experimental  $K_g$  (see eq 2) are very sensitive to the value of  $T_m^\circ$ , at least for data at relatively low  $\Delta T$  as being considered here.  $T_m^\circ$  is frequently estimated from melting points derived from optical microscopy, but these would not generally be expected to be reliable. Experimental melting points ( $T_m$ ) from optical microscopy are generally defined as the temperature at which the last trace of birefringence disappears. Crystalline polymers are well-known to undergo crystal reorganization/thickening during heating, and heating rates on typical hot stages are limited to 10–20 °C/min, frequently too low to inhibit reorganization. Thus, the experimental  $T_m$ 's derived from optical microscopy frequently reflect the melting of the reorganized crystals, not those formed at  $T_c$ .

Consequently, a careful DSC study was undertaken to estimate  $T_m^\circ$  for PBT and the PBT/PAr blends. Isothermally crystallized PBT can exhibit up to four melting endotherms. A relatively low-temperature melting peak is sometimes evident at ca. 5–10 °C above  $T_c$ , whose origin is still unclear.<sup>13</sup> In addition to an endotherm associated with the melting of crystals formed at  $T_c$ , endotherms can also be observed that are associated with melting of crystals formed on cooling from  $T_c$  (usually for samples crystallized at high  $T_c$  for relatively short times) and associated with the melting of material that has reorganized on heating. Irrespective of the method used for estimation of  $T_m^\circ$  (i.e., Hoffman-Weeks or Gibbs-Thomson), care must be taken to select and use the melting point of those crystals formed at  $T_c$ . Within our ability to cool the samples in the DSC, it was determined that isothermal crystallization could be safely conducted for PBT at temperatures in excess of 190 °C. Crystallization was conducted for either 1, 10, or 24 h, and any melting endotherms due to material that crystallized on cooling from  $T_c$  were easily recognized. In fact, crystallization at  $T_c$ 's up to 210 °C was found to be essentially complete within 1 h. The typical melting behavior of PBT crystallized for 10 h over a range of  $T_c$  is shown in Figure 2. From heating rate experiments, the two endotherms seen at low  $T_c$  appear to be a result of a melting, reorganization, and remelting process. Figure 3 shows the results of a heating rate study on PBT crystallized at 200 °C for 1 h. Here, one also sees a third endotherm ca. 10 °C above  $T_c$  as discussed earlier (its location is crystallization time dependent—it moves to higher temperature with increasing time—and is consequently not resolved in Figure 2). The ratio of the first to second prominent endotherms increases as the heating rate increases, consistent with a mechanism based on melting, recrystallization, and subsequent remelting.<sup>14,15</sup> The melting behavior seen in Figure 2 is also consistent

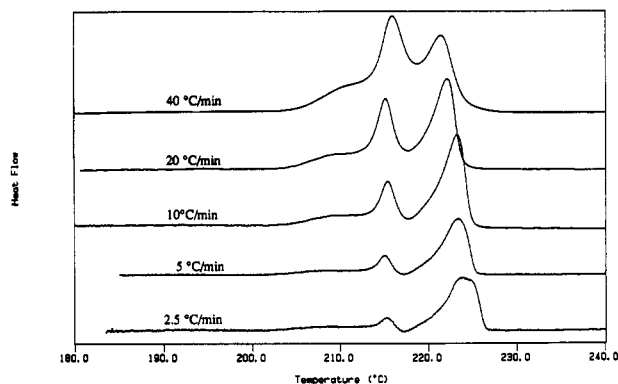


Figure 3. Melting behavior of PBT isothermally crystallized at 200 °C for 1 h at different heating rates.

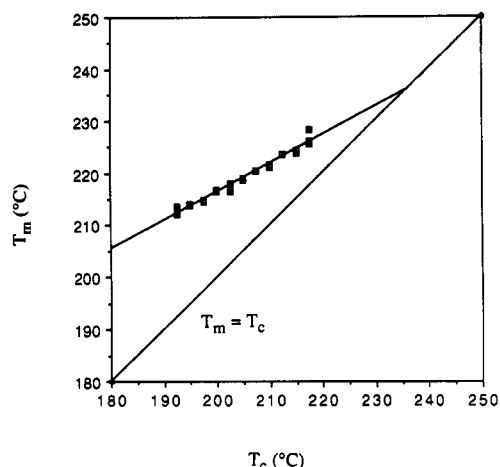


Figure 4. Hoffman-Weeks plot for isothermally crystallized PBT (10-h crystallization).

with this mechanism; crystallization at higher  $T_c$  results in thicker crystals and less propensity for reorganization. The peak temperature of the first (or only) melting endotherm at 20 °C/min was chosen to represent the melting point of the as-crystallized material.

An unusual feature that complicates the determination of experimental melting points in PBT and PBT/PAr blends is that the apparent  $T_m$  is a function of crystallization time through at least 10 h and up to as much as 24 h in the case of PBT. The origin of this behavior is not entirely clear at present and is currently under investigation. The equilibrium melting point was determined for PBT using the Hoffman-Weeks approach (i.e., extrapolation of a plot of  $T_m$  vs  $T_c$  to  $T_m = T_c$ ) for samples crystallized at 1, 10, and 24 h. The  $T_m$ 's derived from the 1- and 10-h experiments were the same within experimental error, and we focus here on the samples crystallized for 10 h. The results of the 24-h experiments will be reported shortly. It should be emphasized that small sample sizes were used to determine experimental melting points due to problems with thermal lag. In fact, in a series of experiments on PBT crystallized at 200 °C for 24 h it was found that the location of the single melting endotherm was ca. 2 °C higher for samples ~4 mg in size versus those of ~0.5 mg. Below 0.5 mg,  $T_m$  was independent of size and the same within error as the extrapolated  $T_m$  at zero sample weight. In the case where a sample exhibits multiple melting endotherms, loss of peak resolution can also occur for the "usual" (5–15 mg) sample sizes.

The melting points (10-h crystallization) are shown in Figure 4 extrapolated to a value of  $T_m^\circ = 236$  °C, in line with the value determined by Wegner<sup>16</sup> from extrapolation of melting data of PBT oligomers. Our value obtained

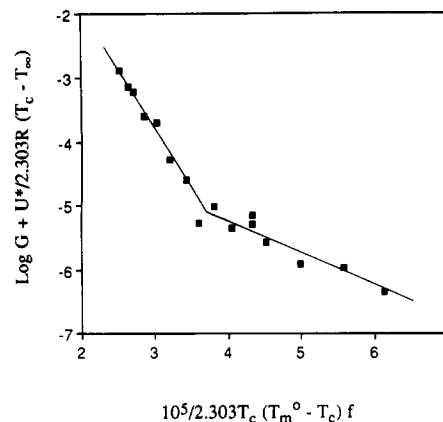


Figure 5. Growth rate data for PBT.

from the DSC experiments should be contrasted with an apparent value of ~260 °C which was obtained by us from extrapolated  $T_m$ 's from optical microscopy.

In the calculations which follow, a  $T_g$  of 42 °C was used for PBT as determined by DSC. Figure 5 shows the growth rate data for PBT plotted according to indications of eq 3. It appears reasonable to fit the experimental data with two straight lines, and the change in slope qualitatively indicates a change in the crystallization regime in the vicinity of 210–212 °C (i.e., from regime II → III). However, the ratio of the derived nucleation constants (Table I) from the separate straight line portions deviates significantly from the theoretical value of  $K_g(\text{III})/K_g(\text{II})$  (i.e., a value of 2 vs ~3.5 obtained experimentally). [To force  $K_g(\text{III})/K_g(\text{II}) \sim 2$  would require a  $T_m^\circ$  near 260 °C, well outside the uncertainty of our  $T_m^\circ$  derived from DSC melting points.] The origin of this deviation is unclear but could be partially associated with the greater experimental uncertainty in the growth rate data at  $T_c$ 's greater than ~210 °C. In order to further investigate if the data at higher  $T_c$  are consistent with regime II crystallization kinetics, we employed the Lauritzen  $Z$  test.<sup>17</sup>  $Z$  is defined as

$$Z \approx 10^3 (L/2a)^2 \exp[-X/T_c \Delta T] \quad (4)$$

where  $L$  is the effective substrate length and  $a$  is the chain stem width (estimated to be 3.82 Å). Regime I kinetics are followed if substitution of  $X = K_g$  into eq 4 results in  $Z \leq 0.01$ . If with  $X = 2K_g$ , eq 4 yields  $Z \geq 1$ , then regime II kinetics are followed. Between these extremes is a test for "regime I within 10 percent" assuming  $Z = 0.1$  and  $X = K_g$ . In practice, it is more convenient to perform the  $Z$  test by using the known value of  $K_g$  and the inequalities for  $Z$  in order to estimate the range of  $L$  values in regime I or regime II. The regime of crystallization is then determined by deciding whether or not the range of  $L$  values calculated in each case is reasonable. The difficulty, however, is assessing what is a reasonable value of  $L$ . Even for polyethylene, estimates for  $L$  at the regime I → II transition have changed over the past few years as both the experimental data and theory have been refined.<sup>18–20</sup> (A value of within about a factor of 3 of 200 Å is the most recent estimate.)<sup>19</sup> Similar estimates of  $L$  for other polymers have not been undertaken. Thus, the guidelines for deciding on regime I or II behavior are ill-defined. Only where particular solutions produce very small or very large  $L$ 's can estimates be made.

Testing the data at high  $T_c$  for conformity to regime I results in a required substrate length of less than 1 Å, which is clearly unrealistic. Testing for regime II requires  $L$  to be greater than 40 Å, at low  $T_c$  and greater than about 390 Å at high  $T_c$ . If the typical substrate length for PBT

is similar to polyethylene, then the calculated values for the Lauritzen  $Z$  parameter are consistent with regime II kinetics at high  $T_c$ .

The derived  $K_g$ 's can be used to calculate  $\sigma_e$  (and the work of chain folding ( $q$ )) for PBT from eq 3. If we assume folding along (010) planes,<sup>21,22</sup> then the layer thickness  $b$  is estimated to be 5.17 Å. Using the value of  $T_m^\circ$  noted earlier and  $\Delta H_f^\circ = 142 \text{ J/g}$ ,<sup>23</sup> we derive the  $\sigma\sigma_e$  product. The primary difficulty in determining  $q$  (via  $\sigma_e$ ) is the difficulty in estimating the lateral surface free energy,  $\sigma$ . The usual approach is to estimate  $\sigma$  from the Thomas-Stavely relationship<sup>3</sup>

$$\sigma = \alpha \Delta H_f^\circ (ab)^{1/2} \quad (5)$$

where  $\alpha$  is an empirical constant.  $\alpha$  is usually assumed to be  $\sim 0.1$ , but very recent work<sup>24</sup> has suggested that there are two classes of polymers: one where  $\alpha = 0.1$  (e.g., polyolefins) and another where  $\alpha = 0.25$  (e.g., poly(pivalolactone)<sup>24</sup> and poly(phenylene sulfide)<sup>25</sup>). At this juncture, however, it is not possible to predict the appropriate  $\alpha$ , given a chemical structure. Therefore, the tack that we took was to calculate  $\sigma$ ,  $\sigma_e$ , and  $q$  using both values, assessing which (if either) produces clearly more reasonable values.  $\sigma_e$  and  $q$  calculated with  $\alpha = 0.25$  are unrealistically small (i.e.,  $q \sim 1 \text{ kcal/mol}$ ), and only values derived with  $\alpha = 0.1$  will be discussed. The work of chain folding can be derived from  $\sigma_e$  by<sup>26</sup>

$$\sigma_e = q/2ab + \sigma_{e0} \quad (6)$$

where  $\sigma_{e0}$  is the value that the surface free energy would assume if no work were required to form a fold.  $\sigma_{e0}$  is usually assumed to be zero (or in another approximation it is assumed to be equal to  $\sigma$ ) and hence can frequently be neglected compared to the first term on the right-hand side of eq 6.

Taking  $\alpha = 0.1$ ,  $\sigma$  was estimated to be  $8.8 \text{ erg/cm}^2$  from eq 5, and using the experimental  $K_g$  derived from the higher quality low- $T_c$  (regime III) growth rate data leads to  $\sigma_e = 57 \text{ erg/cm}^2$ . The work of chain folding has been found to be the one parameter most closely correlated with molecular structure, and probably the most important contribution to its relative magnitude is thought to be the inherent stiffness of the chain itself.<sup>3</sup> For example, polymers with flexible chains such as polyethers have values of  $q$  near 3–4 kcal/mol<sup>3,27</sup> and intermediate ones (e.g., polyethylene and poly(caprolactone) (PCL)) have  $q$  values close to 5 kcal/mol,<sup>20,28</sup> while stiffer ones (e.g., isotactic polystyrene and poly(phenylene sulfide)) have  $q$ 's in the range of 7–9 kcal/mol.<sup>3,25</sup> The calculated work of chain folding for PBT corresponding to  $\sigma_e = 57 \text{ erg/cm}^2$  is surprisingly small—on the order 3 kcal/mol. Recall that we found the PBT melting point at a given  $T_c$  to increase with crystallization time up to  $\sim 24 \text{ h}$  (similar behavior has been reported recently by Phillips and Rensch for PCL<sup>29</sup>). The  $T_m^\circ$  of  $\sim 236^\circ \text{C}$  was determined from extrapolation of melting points acquired at a crystallization time of 10 h. A similar value was obtained for samples that had been crystallized for 1 h. However,  $T_m$ 's for samples crystallized at 24 h are in general somewhat larger, resulting in  $T_m^\circ \sim 244^\circ \text{C}$  (this value is similar to that estimated in two previous publications<sup>30,31</sup>). Analyzing the growth rate data using this  $T_m^\circ$  results in a regime II  $\rightarrow$  III transition in the same location as noted earlier,  $K_g\text{-(III)}/K_g\text{-(II)}$  still considerably different than the theoretical value of 2, but  $\sigma_e = 75 \text{ erg/cm}^2$  ( $q \sim 5 \text{ kcal/mol}$ ). Thus it is clear that the derived  $q$  is very sensitive to the value of  $T_m^\circ$  used in the calculations. Considering the relative uncertainty in  $T_m^\circ$  ( $236\text{--}244^\circ \text{C}$ ), we conclude that  $\sigma_e$  and

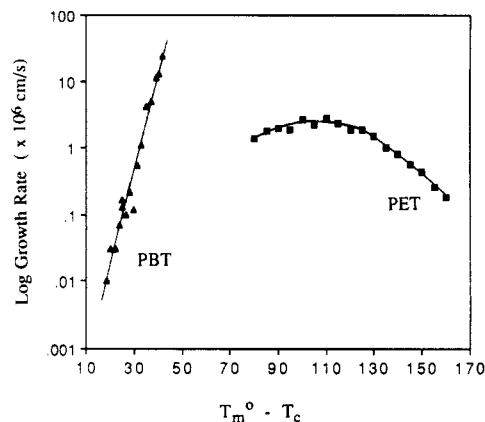


Figure 6. Spherulitic growth rate versus degree of supercooling for PBT and for PET ( $\bar{M}_n = 39\,100$ ). The PET data were taken from ref 32.

$q$  for PBT are in the range of  $\sim 57\text{--}75 \text{ erg/cm}^2$  and 3–5 kcal/mol, respectively. This latter value is somewhat small, perhaps indicating the relative importance of the tetramethylene units in determining the work associated with chain folding.

**B. Comparison with Poly(ethylene terephthalate).** It is well-known that PBT crystallizes more rapidly than poly(ethylene terephthalate) (PET) although the origin of this behavior remains an open question. Figure 6 shows spherulitic growth rates for PBT (determined here) as a function of the degree of supercooling plotted along with growth rates determined by van Antwerpen and van Krevelen<sup>32</sup> for a PET of similar  $\bar{M}_n$  (i.e.,  $\sim 39\,100$ ). Note that the maximum spherulitic growth rate for this PET (at  $\sim 180^\circ \text{C}$ ) is  $\sim 1.5 \mu\text{m/min}$  while the growth rate for PBT of comparable molecular weight is an order of magnitude higher, even at a temperature ( $198^\circ \text{C}$ ) which is likely quite distant from the temperature of maximum growth (which is expected to be roughly midway between  $T_g$  and  $T_m^\circ$ ). As seen in Figure 6, there is considerable PET growth rate data at low  $T_c$  and this permits analysis of the best fit for  $U^*$  and  $T_\infty$ . Using only the data points at the largest  $\Delta T$  and a similar approach to that described by Lovinger et al.,<sup>25</sup> if  $T_\infty$  is assumed to be  $T_g - 30^\circ \text{C}$ , the best linear fit of the low- $T_c$  data is with  $U^* \sim 1500 \text{ cal/mol}$ , i.e., the universal value. In fact, when both  $U^*$  and  $T_\infty$  are permitted to vary, the highest correlation coefficient was obtained when  $U^*$  and  $T_\infty$  take on values near the universal values.

For PET,  $T_m^\circ$  and  $\Delta H_f^\circ$  have been determined to be  $280^\circ \text{C}$  and  $140 \text{ J/g}$ , respectively.<sup>33</sup>  $T_g$  was taken to be  $75^\circ \text{C}$ . Palys and Phillips have taken the monomolecular layer thickness as the perpendicular separation of (010) planes and arrived at  $b = 5.53 \text{ Å}$  and  $a = 4.56 \text{ Å}$ .<sup>34</sup> Figure 7 shows the growth rate data for PET ( $\bar{M}_n = 39\,100$ ) as well as data for two samples of lower molecular weight reported in ref 32, according to the indications of eq 3. Best fit values for  $K_g$  and  $G_0$  are provided in Table II. Note that, with  $U^* \sim 1500 \text{ cal/mol}$ , no regime transition is evident in this experimental data, in contrast to a recent report.<sup>35</sup> Results of the Lauritzen  $Z$  test preclude crystallization in regime I (i.e.,  $L$  would need to be less than a few angstroms) and generally support the idea that the crystallization follows regime II kinetics over the entire  $T_c$  range ( $L$  is calculated to be greater than a few tens of angstroms at the lowest  $T_c$  and a few thousand angstroms at the highest  $T_c$ ).

For crystallization in regime II the  $\sigma\sigma_e$  product was found to be  $1510 \text{ erg}^2/\text{cm}^4$  for the polymer with  $\bar{M}_n = 39\,100$ . The difficulty again is deciding on a realistic value for  $\alpha$ .  $\alpha$  for

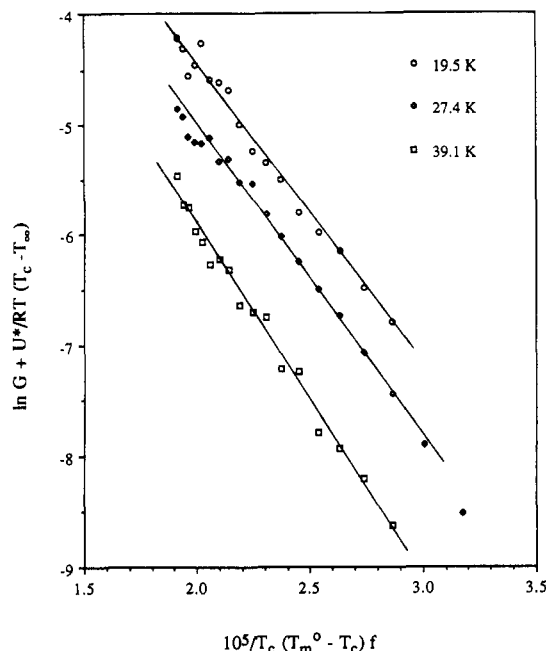


Figure 7. Growth rates for PET of  $\bar{M}_n = 19\,500$ ,  $27\,400$ , and  $39\,100$  (data from ref 32).

Table II  
Nucleation Constants and Preexponential Factors for PET<sup>a</sup>

$\bar{M}_n \times 10^{-3}$	$K_g \times 10^{-5} (K^2)$	$G_0, \text{cm/s}$
19.5	2.76	2.95
27.4	2.81	1.80
39.1	3.16	1.49

<sup>a</sup> Derived from data in ref 32.

PBT was found to be 0.1, and we would not expect the value for PET to be much different. With this assumption we arrive at  $\sigma = 10.6 \text{ erg/cm}^2$  (from the Thomas-Stavey relationship),  $\sigma_e \sim 140 \text{ erg/cm}^2$ , and  $q \sim 10 \text{ kcal/mol}$ . These latter two values are about a factor of 2 larger than those derived for PBT. Provided these estimates are reasonable, this provides some interesting insight into the nature of the differences in the crystallization kinetics of PET and PBT. It has been well established that crystal substrate completion (i.e., crystal growth) is retarded by the necessity for forming folds and reptation in the melt.<sup>20,36</sup> At low  $\Delta T$ , once the regime is fixed, the work of chain folding has been found to be the most important parameter governing the temperature dependence of the growth rate. From our estimates above it appears that the work required to form a PBT fold is roughly half of that for PET, and hence chain folding is less of a hindrance to crystallization for PBT. This relatively large difference in  $q$  is apparently associated with the longer flexible segments (i.e.,  $(\text{CH}_2)_4$  vs  $(\text{CH}_2)_2$ ) in the PBT repeat unit. All other parameters being equal, entrance of PBT into regime III growth (i.e., very rapid nucleation at the crystal growth front) would also result in an increase in the growth rate.

**C. PBT/PAr Blends.** There are two approaches which can be taken to analyze the growth rate data for the blends. The phenomenological equation proposed by Alfonso and Russell<sup>37</sup> has proven quite successful for analyzing the crystallization kinetics of miscible poly(ethylene oxide)/poly(methyl methacrylate) blends but is relatively difficult to utilize because parameters such as the polymer-polymer interaction parameter,  $\chi$ , and the mutual diffusion coefficient are often not well established. As this is the case here also, we analyzed the growth rate data for the PBT/

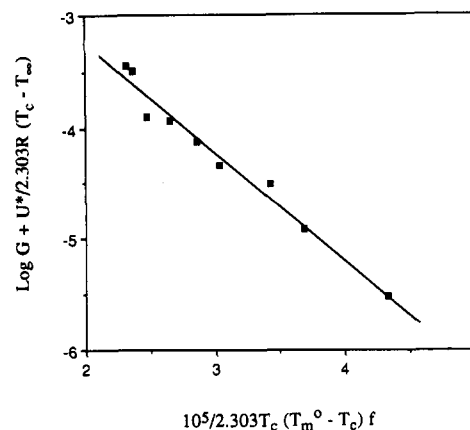


Figure 8. Growth rate data for PBT/PAr (80/20) blend.

PAr blends in a similar fashion to PBT and PET. A modified Lauritzen-Hoffman expression for the growth rate can be written as

$$G = G_0' \exp[-U^*/R(T_c - T_\infty)] \exp[-K_g'/T_c(\Delta T)f] \quad (7)$$

where  $G_0' = V_2 G_0$  ( $V_2$  is the volume fraction of the crystalline polymer), to account for the proportionality between the rate of nucleation and concentration of crystallizable units. The modified nucleation constant can be written as<sup>38</sup>

$$K_g' = nb\sigma\sigma_e T_{mb}^0 / \Delta H_f^0 k - 2\sigma T_c T_{mb}^0 \ln V_2 / b\Delta H_f^0 \quad (8)$$

where  $T_{mb}^0$  is the equilibrium melting point of PBT in the blend. The second term arises from an entropic contribution to the free energy required to form a nucleus of critical size. In our case, the second term ranges from only about 2 to 8% of the first and is therefore neglected in our analysis. The growth rate data for one of the blends [i.e., PBT/PAr (80/20)], represented in similar fashion to Figures 5 and 7 is shown in Figure 8. In general, the data for all blends are best fit by a single straight line. Application of the Lauritzen  $Z$  test appears to rule out crystallization in regime I, although it is difficult to determine whether the data conform to regime II or III. The  $T_c$  range covered for the blends generally falls in the range that was associated with regime III for PBT. However,  $L$ 's derived from the Lauritzen  $Z$  test are consistent with regime II at low  $T_c$  and using the lower end of the estimated  $T_m^0$  range (but they are quite large at high  $T_c$ ). The difficulty is there is no way to test directly for regime III. Following from PBT, we will assume regime III kinetics in what is to follow. Equilibrium melting points for PBT in the blends were determined by extrapolating Hoffman-Weeks plots, and  $T_m^0$ 's for all three blends were found to be within  $\sim 2^\circ\text{C}$  of the value for PBT, i.e., the same within experimental error.  $T_g$ 's for all blends were estimated from DSC. Assuming  $T_m^0 = 236^\circ\text{C}$  leads to  $\sigma_e$  for the blends in the range of  $30\text{--}50 \text{ erg/cm}^2$ , while taking  $T_m^0 = 244^\circ\text{C}$  results in  $\sigma_e \sim 50\text{--}80 \text{ erg/cm}^2$ . These values are generally somewhat lower than that derived for PBT, but it is premature to conclude any fundamental change in the nature of the chain folding in the blends because of the uncertainty in the crystallization regime and relatively limited growth rate data available.

**Acknowledgment.** We express our appreciation to Hoechst Celanese Corp., particularly Dr. Thomas Dolce, for their support of this research.

## References and Notes

- (1) Runt, J.; Barron, C. A.; Zhang, X.; Kumar, S. K. *Macromolecules* 1991, 24, 346.

- (2) Runt, J.; Miley, D. M. *Polym. Commun.* Submitted for publication.
- (3) Hoffman, J. D.; Davis, G. T.; Lauritzen, J. I. In *Treatise on Solid State Chemistry*; Hannay, H. B., Ed.; Plenum: New York, 1975; Vol. 3.
- (4) Borman, W. F. H. *J. Appl. Polym. Sci.* **1978**, *22*, 2119.
- (5) Private communication from Dr. Paul Chen, Hoechst Celanese Corp.
- (6) Kimura, M.; Porter, R. S.; Salee, G. J. *Polym. Sci., Polym. Phys. Ed.* **1983**, *21*, 367.
- (7) Iruin, J.; Equiazabal, J. I.; Guzman, G. M. *Eur. Polym. J.* **1989**, *25*, 1169.
- (8) Runt, J.; Harrison, I. R. In *Methods of Experimental Physics*; Fava, R., Ed.; Academic Press: New York, 1980; Vol. 16B, Chapter 9.
- (9) Gilbert, M.; Hybart, F. J. *Polymer* **1972**, *13*, 327.
- (10) Wasiak, A.; Stein, R. S. *Polym. Prepr. (Am. Chem. Soc., Div. Polym. Chem.)* **1975**, 643.
- (11) Piacella, M.; Chiellini, E.; Dainelli, D. **1989**, *190*, 175.
- (12) Hoffman, J. D.; Miller, R. L. *Macromolecules* **1989**, *22*, 3505.
- (13) Yeh, J. T.; Runt, J. *J. Polym. Sci., Polym. Phys. Ed.* **1989**, *27*, 1543.
- (14) Rim, P. B.; Runt, J. *Macromolecules* **1983**, *26*, 762.
- (15) Harrison, I. R.; Landes, B. *J. Macromol. Sci., Phys.* **1983**, *22*, 747.
- (16) Wegner, G. In *Thermoplastic Elastomers*; Legge, N. R., Holden, G., Schroeder, H. E., Eds.; Hanser: New York, 1989.
- (17) Lauritzen, J. I. *J. Appl. Phys.* **1973**, *44*, 4353.
- (18) Hoffman, J. D. *Polymer* **1985**, *26*, 803.
- (19) Hoffman, J. D.; Miller, R. L. *Macromolecules* **1989**, *22*, 3502.
- (20) Hoffman, J. D.; Miller, R. L. *Macromolecules* **1988**, *21*, 3038.
- (21) Briber, R. M.; Thomas, E. L. *Polymer* **1985**, *26*, 8.
- (22) Briber, R. M.; Thomas, E. L. *Polymer* **1986**, *27*, 66.
- (23) Illers, K. H. *Colloid Polym. Sci.* **1980**, *258*, 117.
- (24) Roitman, D. B.; Marand, H.; Miller, R. L.; Hoffman, J. D. *J. Phys. Chem.* **1989**, *93*, 6929.
- (25) Lovinger, A. J.; Davis, D. D.; Padden, F. J. *Polymer* **1985**, *26*, 1595.
- (26) Lauritzen, J. I.; Hoffman, J. D. *J. Res. Natl. Bur. Stand., Sect. A* **1960**, *64A*, 73.
- (27) Runt, J.; Wagner, R. F.; Zimmer, M. *Macromolecules* **1987**, *20*, 2531.
- (28) Phillips, P. J.; Rensch, G. J.; Taylor, K. D. *J. Polym. Sci., Polym. Phys. Ed.* **1987**, *25*, 27.
- (29) Phillips, P. J.; Rensch, G. J. *J. Polym. Sci., Polym. Phys. Ed.* **1989**, *27*, 155.
- (30) Cheng, S. Z. D.; Pan, R.; Wunderlich, B. *Macromol. Chem.* **1988**, *189*, 2443.
- (31) Pracella, M.; Chielinni, E.; Dainelli, D. *Macromol. Chem.* **1989**, *190*, 175.
- (32) van Antwerpen, F.; van Krevelen, D. W. *J. Polym. Sci., Polym. Phys. Ed.* **1972**, *10*, 2423.
- (33) Wunderlich, B. *Macromolecular Physics*; Academic Press: New York, 1980; Vol. 3.
- (34) Palys, L. H.; Phillips, P. J. *J. Polym. Sci., Polym. Phys. Ed.* **1980**, *18*, 829.
- (35) Phillips, P. J.; Tseng, H. T. *Macromolecules* **1989**, *22*, 1649.
- (36) Hoffman, J. D. *Polymer* **1985**, *26*, 803.
- (37) Alfonso, G. C.; Russell, T. P. *Macromolecules* **1986**, *19*, 1143.
- (38) Boon, J.; Azcue, J. M. *J. Polym. Sci., Polym. Phys. Ed.* **1968**, *6*, 885.

**Registry No.** PBT (copolymer), 26062-94-2; PBT (SRU), 24968-12-5; bisphenol A-isophthalic acid-terephthalic acid (copolymer), 26590-50-1; bisphenol A-isophthalic acid-terephthalic acid (SRU), 39281-59-9.